


Synaptic changes modulate spontaneous transitions between tonic and bursting neural activities in coupled Hindmarsh-Rose neurons

Jian-Fang Zhou,¹ En-Hua Jiang,¹ Bang-Lin Xu,¹ Kesheng Xu,² Changsong Zhou,^{3,*} and Wu-Jie Yuan^{1,†}

¹College of Physics and Electronic Information, Huaibei Normal University, Huaibei 235000, China

²College of Science, Jiangsu University, Zhenjiang 212000, China

³Department of Physics, Centre for Nonlinear Studies, Institute of Computational and Theoretical Studies, Hong Kong Baptist University, Kowloon Tong 999077, Hong Kong, China

 (Received 25 September 2020; revised 27 August 2021; accepted 26 October 2021; published 15 November 2021)

Experimentally, certain cells in the brain exhibit a spike-burst activity with burst synchronization at transition to and during sleep (or drowsiness), while they demonstrate a desynchronized tonic activity in the waking state. We herein investigated the neural activities and their transitions by using a model of coupled Hindmarsh-Rose neurons in an Erdős-Rényi random network. By tuning synaptic strength, spontaneous transitions between tonic and bursting neural activities can be realized. With excitatory chemical synapses or electrical synapses, slow-wave activity (SWA) similar to that observed during sleep can appear, as a result of synchronized bursting activities. SWA cannot appear in a network that is dominated by inhibitory chemical synapses, because neurons exhibit desynchronized bursting activities. Moreover, we found that the critical synaptic strength related to the transitions of neural activities depends only on the network average degree (i.e., the average number of signals that all the neurons receive). We demonstrated, both numerically and analytically, that the critical synaptic strength and the network average degree obey a power-law relation with an exponent of -1 . Our study provides a possible dynamical network mechanism of the transitions between tonic and bursting neural activities for the wakefulness-sleep cycle, and of the SWA during sleep. Further interesting and challenging investigations are briefly discussed as well.

DOI: [10.1103/PhysRevE.104.054407](https://doi.org/10.1103/PhysRevE.104.054407)

I. INTRODUCTION

Certain cells in the brain (e.g., in the thalamus) exhibit a spike-burst activity (repeating sequences of multiple spikes) with burst synchronization at transition to and during sleep (or drowsiness), while they show a desynchronized tonic activity (rhythmic single spiking) during the waking state [1–4]. Such a spike-burst activity behaves experimentally as a multi-timescale phenomenon with a slow process (burst), modulating a fast, repetitive, firing (spike) pattern. The slow (<1 Hz) oscillations observed in the electroencephalographic recordings of naturally sleeping humans and other mammals, are considered to be the result of the synchronized spike-burst activity of neurons in the brain [4,5]. So far, there have been many models of thalamocortical slow-wave sleep oscillations [6,7], that suggest that the aforementioned oscillations arise from an interaction between cortical and thalamic circuits. In the network models, the constructed neuronal links are particularly complex. For example, the model in Ref. [6] was constructed according to a large number of physiological and anatomical constraints and includes more than 30 000 spiking neurons interconnected by more than 5×10^6 synaptic connections and organized hierarchically into three cortical areas with columnar connections including five cortical layers. In

Ref. [7], the network model consisted of a one-dimensional four-layer array of N pyramidal neurons, $N/4$ interneurons, and $N/2$ reticular and $N/2$ thalamocortical neurons with different AMPA-, NMDA-, GABA_A-, and GABA_B-mediated synapses. Although the network models can produce slow-wave oscillations by tuning parameters of neuronal dynamics for the induction of the sleep state, the underlying network mechanism of the tonic-to-burst transition and the resulting slow-wave activity (SWA) with burst synchronization remains unclear.

On the other hand, a wide range of human and animal studies have found that net synaptic strength in neural networks increases during wakefulness and returns to a baseline level during sleep [8–10]. Moreover, these changes in synaptic strength are accompanied by corresponding changes in neural dynamics (including tonic and burst activities) and sleep SWA [11–13], and the SWA may reflect synaptic changes underlying a cellular need for sleep [13,14]. Based on the experimental evidence including the changes in neural activity and synaptic strength for the wakefulness-sleep cycle, one can extrapolate two key and essential transition processes of neural dynamics for the cycle. The first transition is that the desynchronized tonic activity in wakefulness can change into the spike-burst activity with burst synchronization, thus producing the sleep SWA with an increasing of synaptic strength. The second transition is that the spike-burst activity during sleep can return to the desynchronized tonic activity of the waking state when the increased synaptic strength decreases

*cszhou@hkbu.edu.hk

†yuanwj2005@163.com

to a baseline level. Obviously, there is an association between synaptic changes and neural dynamical transitions. So far, the causal relationship of the association has been, experimentally and theoretically, unclear. Based on the association, we hereby assume that the neuronal spiking patterns result from synaptic changes in the neural network, although the spiking pattern of a single neuron might be due to modulations of the intrinsic ionic (e.g., sodium and potassium) channel conductance during the wakefulness-sleep cycle [6]. In this paper, we wonder whether the network coupling only under the changes of synaptic strength (that does not take into account the interaction between cortical and thalamic circuits) could contribute to the dynamical transitions at both the neuronal (tonic-burst) and the network (SWA) levels. Our aim is to provide a computational study that would investigate the dynamical transitions similar to those observed throughout the wakefulness-sleep cycle, and to focus on the transitions' dependence on synaptic strength by using a simple neural network model.

II. MODEL

We consider a network model of N coupled Hindmarsh-Rose (HR) neurons [15] with chemical or electrical synapses. In the chemically coupled network, the dynamics of neuron i can be described by the following equations:

$$\begin{aligned} \dot{x}_i &= y_i - ax_i^3 + bx_i^2 - z_i + I_{\text{ext}} \\ &+ g \sum_{j=1, j \neq i}^N A_{ij}(V_s - x_i)G_j, \end{aligned} \quad (1)$$

$$\dot{y}_i = c - dx_i^2 - y_i, \quad (2)$$

$$\dot{z}_i = r[s(x_i - x_0) - z_i]. \quad (3)$$

In Eq. (1), we let the reversal potential $V_s = 2$ (which is always larger than $x_i(t)$ for all the neurons i at any time t), i.e., the chemical synapses are excitatory. The reversal potential $V_s = -1.7$ [which is always smaller than $x_i(t)$] denotes that the chemical synapses are inhibitory. G_j is the synaptic conductance of a presynaptic neuron j , which is modeled as an exponentially decaying function [16,17]. When the neuron j fires, the synaptic conductance is increased, $G_j \rightarrow G_j + \Delta G_{\text{ex}}$ (or $G_j \rightarrow G_j + \Delta G_{\text{inh}}$) for the excitatory (or inhibitory) synapse of neuron j . Otherwise, it decays exponentially with a time constant τ_{ex} (or τ_{inh}) for the excitatory (or inhibitory) synapse. For the electrically synaptic coupled network, only Eq. (1) in the above Eqs. (1)–(3) needs to be replaced with

$$\begin{aligned} \dot{x}_i &= y_i - ax_i^3 + bx_i^2 - z_i + I_{\text{ext}} \\ &+ g \sum_{j=1, j \neq i}^N A_{ij}(x_j - x_i). \end{aligned} \quad (4)$$

Here, the electrically synaptic coupling is linear and directly dependent on the difference of the membrane potentials [18,19]. In the network, the chemically or electrically coupled model is composed of identical HR neurons [15]. In the above equations, x_i represents the membrane potential, y_i is associated with the fast current, and z_i with the slow current. I_{ext} is an external current. g is the synaptic coupling strength (for simplicity, the same coupling strengths are hereby provided

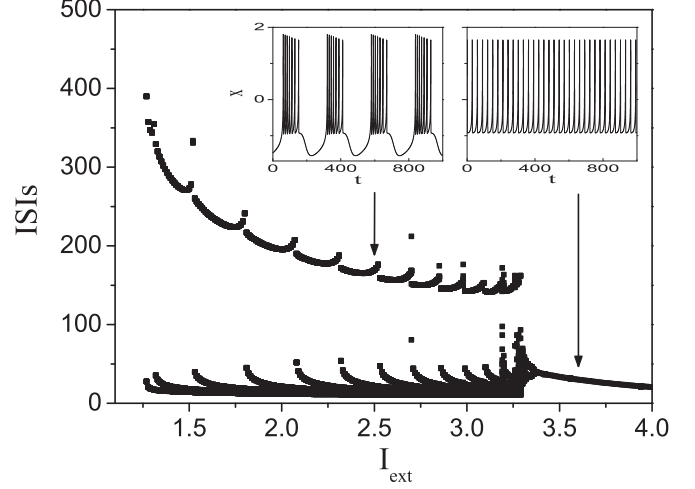


FIG. 1. The diagram of ISIs versus external current I_{ext} for a single HR neuron. The insets show the time series of bursting (at $I_{\text{ext}} = 2.5$) and tonic (at $I_{\text{ext}} = 3.6$) activities of the membrane potential x .

for all synapses). A_{ij} is an element of the adjacency matrix: $A_{ij} = 1$ when a synaptic connection exists from neuron j to i ; otherwise, $A_{ij} = 0$. The $k_i = \sum_{j=1, j \neq i}^N A_{ij}$ is the degree of neuron i , which denotes the number of coupled neurons of the neuron i . The network average degree is defined by $\bar{k} = \frac{1}{N} \sum_{i=1}^N k_i$. The parameters are chosen as follows: $a = 1$, $b = 3$, $c = 1$, $d = 5$, $\gamma = 0.002$, $s = 4$, $x_0 = -1.6$, $\Delta G_{\text{ex}} = \Delta G_{\text{inh}} = 1$, $\tau_{\text{ex}} = 1$, and $\tau_{\text{inh}} = 4$. The single HR neuron can exhibit tonic or bursting activity by tuning I_{ext} . In Fig. 1, we present the interspike intervals (ISIs). The tonic state appears for $I_{\text{ext}} > 3.3$, and a multi-timescale spike-burst behavior for $1.27 < I_{\text{ext}} < 3.3$. In this case, we choose $I_{\text{ext}} = 3.6$, at which a single (or uncoupled) neuron exhibits a tonic activity.

In our network model, the Erdős-Rényi (ER) random network [20] is chosen. For simplicity and comparison between the chemical and the electrical coupling, the adjacency matrix $A = (A_{ij})$ is considered as symmetric (i.e., $A_{ij} = A_{ji}$). In order to describe the collective neuron dynamics, we employ the average membrane potential $\bar{x} = \frac{1}{N} \sum_{i=1}^N x_i$ as the average potential signal of the whole network.

III. RESULTS

In experiments, the potentiation (or depression) of the net synaptic strength in the neural networks seems to be the underlying mechanism of learning (or resting) during wakefulness (or sleep), which is mediated by complicated cascades of cellular events [13,21]. For simplicity, our model uses a linear increase and decrease function for the change of synaptic strength [see Fig. 2(a)]. In Figs. 2(b)–2(f), the two transitions between tonic and bursting neural activities can spontaneously emerge in the chemically coupled network with excitatory synapses by tuning the synaptic strength. The neurons exhibit desynchronized tonic activities in the region of weak synaptic strength [see Fig. 2(b), far left]. With the increasing of synaptic strength [see Fig. 2(a), left half], the spike-burst activities with burst synchronization appear from

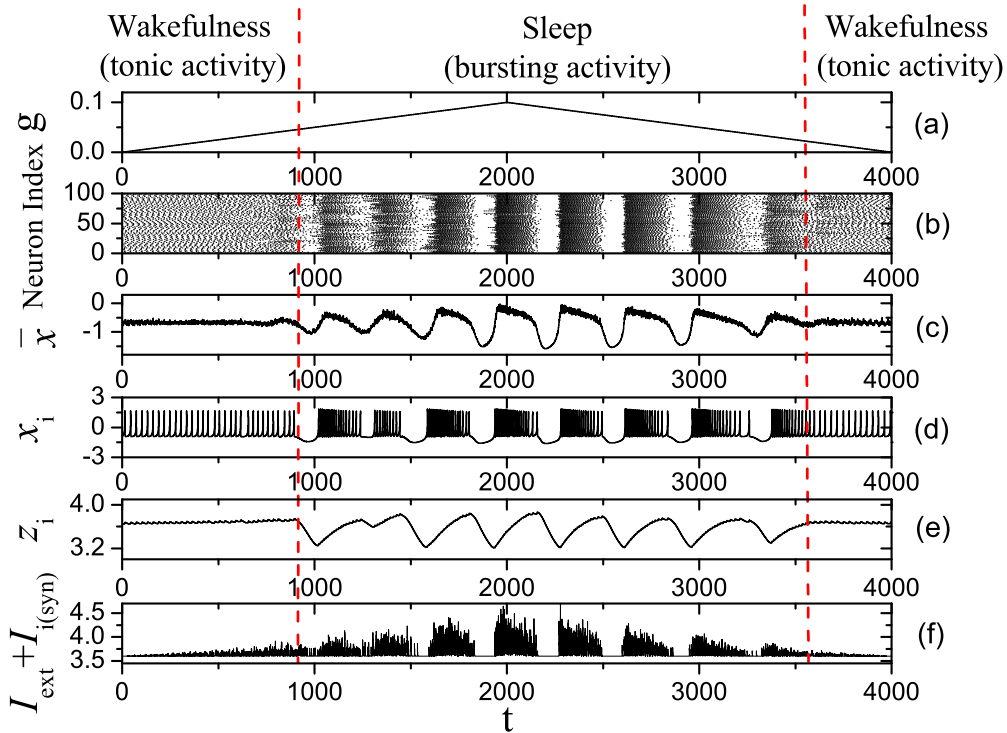


FIG. 2. The two spontaneous transitions between the tonic and the bursting neural activities in an ER random network with size $N = 100$ and excitatory chemical connection probability $p = 0.1$. (a) The change of synaptic strength g . (b) The dot-raster plot showing the firing pattern. (c) The average potential signal \bar{x} of the whole network. (d) The membrane potential x_i and (e) the slow current z_i , and (f) the sum of external current I_{ext} and synaptic coupling current $I_{i(\text{syn})}$ for a randomly chosen neuron i . The two vertical red dashed lines illustrate the critical times of the two transitions.

the tonic activities in the whole network [see Fig. 2(b), left half]. Thus, the potential signal of the whole network can transfer from a low-amplitude, high-frequency fluctuation to a high-amplitude, slow wave [i.e., SWA; see Fig. 2(c), left half], which was experimentally found in electroencephalogram recordings under the states of wakefulness and sleep [22]. In order to understand the emergence of the bursting activity, the membrane potential x_i and the current z_i of a randomly chosen neuron i in the network are provided in Figs. 2(d) and 2(e). It is found that, the bursting activity of the membrane potential x_i emerges due to the appearance of a slow current z_i [see Figs. 2(d) and 2(e), left half], as similarly shown in a single HR neuron [15]. Moreover, we show the sum of the external current I_{ext} and the synaptic coupling current $I_{i(\text{syn})} = g \sum_{j=1, j \neq i}^N A_{ij}(V_s - x_i)G_j$ for the neuron i in Fig. 2(f), in order to compare with the causal role of the external current I_{ext} in a single HR neuron. It is important to stress that the spike-burst activity results from an oscillatory current $I_{\text{ext}} + I_{i(\text{syn})} > I_{\text{ext}} = 3.6$ in the coupled neural network, which is different from the bifurcation to the bursting regime induced by a static current in the range $1.27 < I_{\text{ext}} < 3.3$ as shown in the single HR neuron (see Fig. 1). This indicates that the spike-burst activity is an emergence of collective behavior in the coupled dynamical network. In the latter part of the results, we will study in more detail the neuronal response to oscillatory input in order to reveal the dependence of the spike-burst activity on network connectivity. On the other hand, the bursting-to-tonic transition can also appear

[see Figs. 2(b)–2(f), right half] when the increased synaptic strength decreases to a baseline level [see Fig. 2(a), right half].

From Fig. 2, we can see that two critical values of synaptic strength exist for the two respective transitions. One is approximately $g = 0.046$ (i.e., at $t \approx 910$) with the increasing of synaptic strength, while the other is approximately $g = 0.021$ (i.e., at $t \approx 3580$) with the decreasing of synaptic strength (see the two red dashed lines in Fig. 2). The two critical values are not equal, because of the delay in the network responses to the changes of synaptic strength. The two critical values will be equal to a same value g^* ($0.021 < g^* < 0.046$; result not shown), if there is a long enough time for the changes in synaptic strength (meaning, if the changes of synaptic strength are slow enough). In order to study the critical value g^* of the network, we plot the ISIs of a randomly chosen neuron in the homogeneous ER network as a function of the static synaptic strength g in Fig. 3. In this case, the ISIs are calculated when the response of the network arrives to the stable state under the corresponding synaptic strength. As shown in Fig. 1, the interburst interval is far larger than 100, when the neuron exhibits a spike-burst activity. With the increasing of g , there is a critical value (≈ 0.023) so that if it is exceeded by g , then large ISIs (> 100) illustrating the bursting activity appear in Fig. 3. We define this critical value as the critical g^* . In order to indicate the transition as the boundary of g^* , the dynamical activities of the neuron and the corresponding potential signals of the whole network are shown in the regions of $g < g^*$ and $g > g^*$, respectively (see insets in Fig. 3). Particularly,

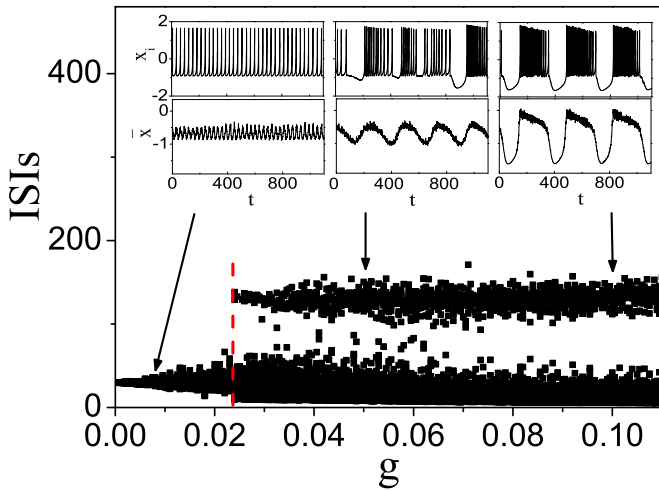


FIG. 3. The diagram of ISIs versus synaptic strength g for a randomly chosen neuron i in the ER random network with a scale of $N = 100$ and an excitatory chemical connection probability $p = 0.1$. The insets demonstrate the time series of the tonic (at $g = 0.008$) and the bursting (at $g = 0.05$ and $g = 0.1$) activities of the membrane potential x_i (top panels) for the chosen neuron i as well as the average potential signal \bar{x} (bottom panels) for the whole network. The vertical red dashed line illustrates the critical g^* producing the transition between the tonic and the bursting activities.

the higher-amplitude, slower wave appears with the further increasing of g , reflecting the state of deep sleep.

For comparison, we perform simulations with electrical synapses in the model. As shown in Figs. 4 and 5, we obtain similar results to those with the excitatory chemical synapses (Figs. 2 and 3). In Fig. 4, the two transitions between the

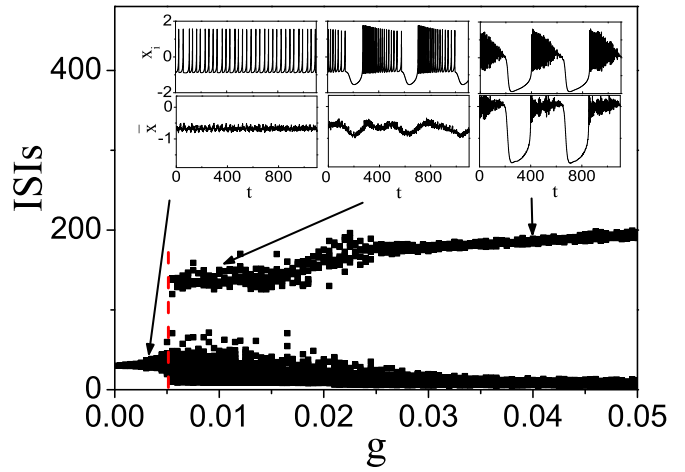


FIG. 5. The same as in Fig. 3, but for an electrically coupled network. The insets are given at $g = 0.003$, $g = 0.01$, and $g = 0.04$.

tonic and the bursting neural activities can spontaneously emerge by tuning synaptic strength g . With the increasing of g , the synchronized bursting activities and the resulting SWA can appear. Moreover, there is a critical synaptic strength g^* for these transitions, shown in Fig. 5. The higher-amplitude, slower wave can also appear with the further increasing of g (see insets in Fig. 5).

In addition, we also perform simulations with inhibitory chemical synapses in the model. In this case, there are also two transitions between the tonic and the bursting neural activities by tuning the synaptic strength (see Fig. 6), and there is also a critical synaptic strength g^* for these transitions (see Fig. 7). The emerging spike-burst activities exhibit desynchronized bursting activities [see Fig. 6(b)] that cannot

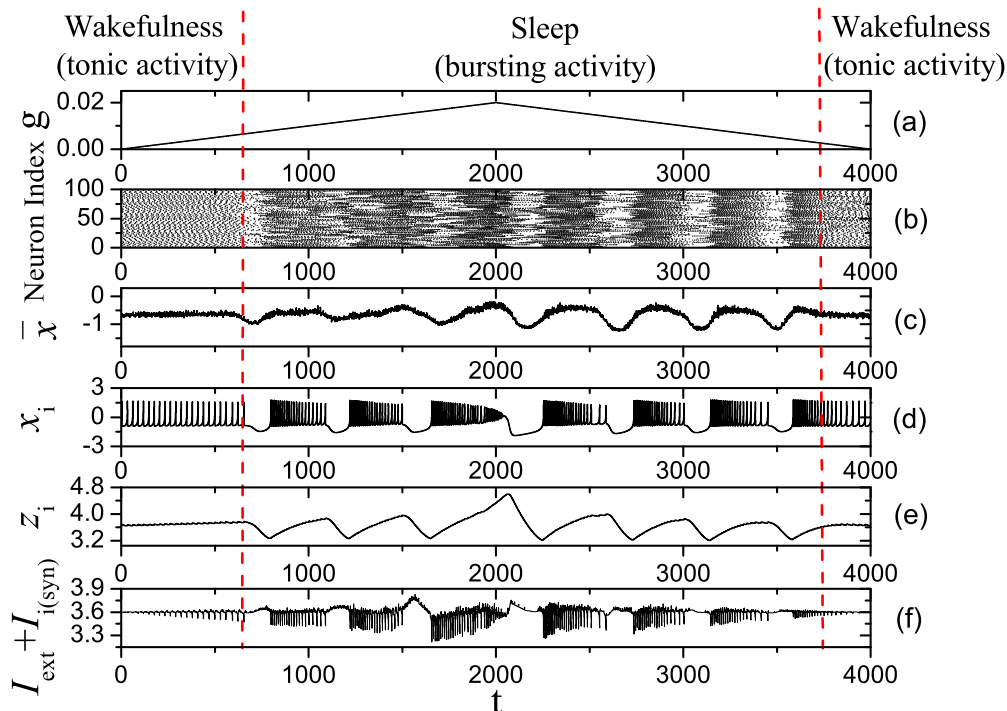


FIG. 4. The same as in Fig. 2, but for an electrically coupled network.

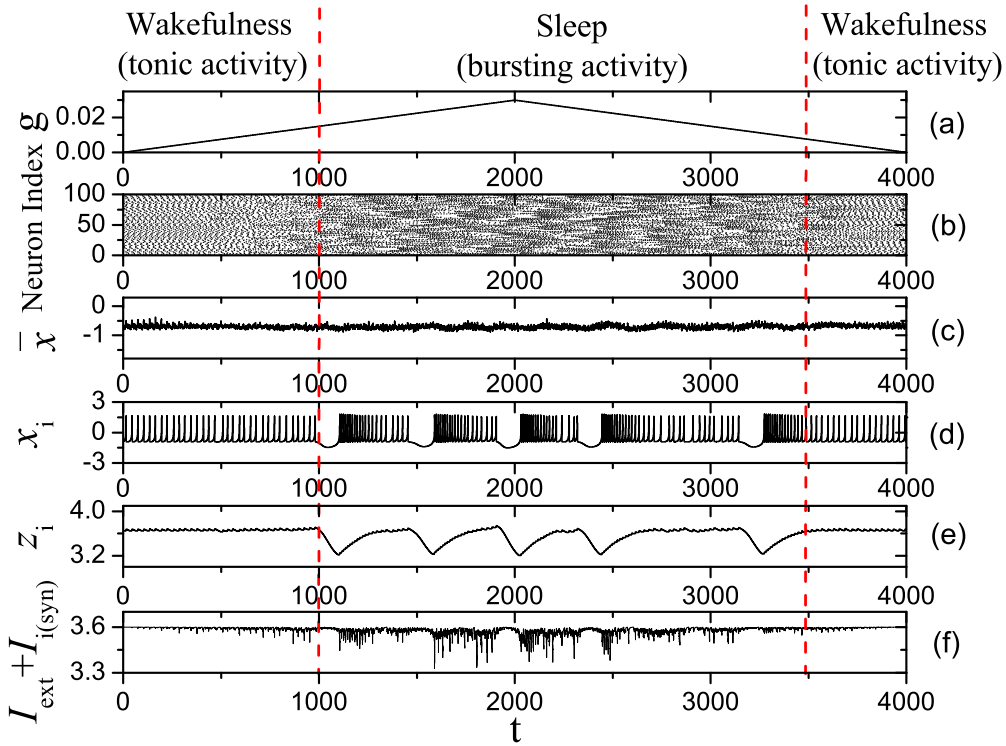


FIG. 6. The same as in Fig. 2, but for inhibitory chemical synaptic connections.

induce a SWA [see Fig. 6(c)]. However, the aforementioned results showed that the synchronized bursting activities and the resulting SWA can appear in the presence of excitatory chemical synapses [see Figs. 2(b) and 2(c)]. The different results obtained between excitatory and inhibitory chemical synapses indicate that the SWA during sleep could be induced mainly by the excitatory chemical synapses; a fact that is consistent with the larger number of excitatory synapses (than that of inhibitory synapses) in realistic neural systems. The bursting activity of the membrane potential x_i emerges due to the appearance of a slow current z_i [see Figs. 6(d) and 6(e)], resulting from an oscillatory current $I_{ext} + I_{i(syn)} < I_{ext} = 3.6$

[see Fig. 6(f)]. In fact, we find that the bursting activities can appear in chemically coupled networks including both excitatory and inhibitory synapses. Whether the synchronized bursting activities and the SWA appear depends on the ratio of excitatory to inhibitory synapses. The synchronized bursting and SWA occur with a high enough ratio (e.g., 4:1, which is about the ratio of excitatory to inhibitory synapses in real neuronal networks; see Fig. 8); otherwise, they do not occur at all (e.g., with a 1:4 ratio; see Fig. 9).

The critical value g^* is key to the transitions between the tonic and the bursting activities in networks with excitatory (or inhibitory) chemical synapses and electrical synapses, respectively. Further below, we focus on the dependence of g^* on network connectivity. In our simulations, we calculate ISIs for all the neurons as a function of synaptic strength g , as in Figs. 3, 5, and 7. As long as there is one neuron transferring from tonic to bursting activity at a certain g , we take the g value as the critical value g^* in the network. The changes of g^* as a function of the network size N for different connection probabilities p are shown in Fig. 10. We conclude that g^* approximately obeys a power-law relation, $g^* \sim N^{-1}$, for different connection probabilities p in chemically and electrically coupled networks. The scaling exponent -1 is independent of p . Moreover, the variation of g^* versus the network average degree $\bar{k} \approx (N - 1)p$ is shown in Fig. 11. The curves obtained for different p in excitatory and inhibitory chemically and electrically coupled networks collapse into a single one, respectively. This indicates that there is a general power-law relation,

$$g^* \sim \bar{k}^{-1}. \tag{5}$$

Thus, g^* is not dependent directly on the network size N and the connection probability p in ER networks. It

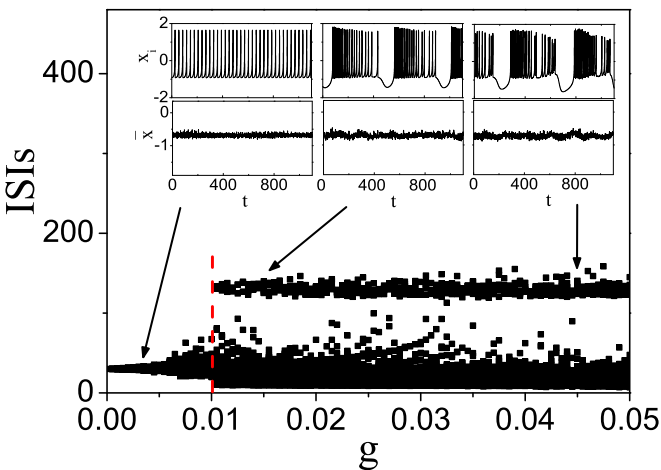


FIG. 7. The same as in Fig. 3, but for inhibitory chemical synaptic connections. The insets are given at $g = 0.003$, $g = 0.015$, and $g = 0.045$.

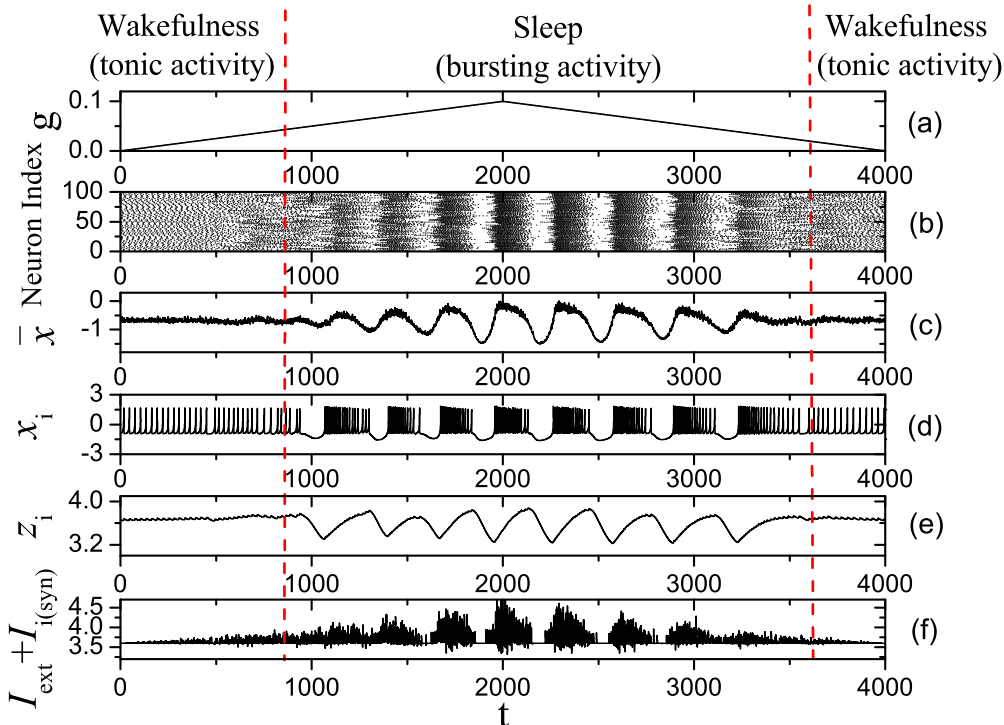


FIG. 8. The same as in Fig. 2, but for a chemically coupled network including both excitatory and inhibitory synapses at a ratio of 4:1.

is only determined by the network average degree \bar{k} , denoting the average number of signals that all the neurons receive. Namely, $g^*\bar{k}$ is a constant corresponding to the tonic-to-bursting transition coupling threshold. One can note

that in Fig. 11, g^* with excitatory synapses is slightly larger than that with inhibitory synapses for the same \bar{k} in a chemically coupled network. Additionally, g^* with inhibitory synapses in a chemically coupled network is slightly

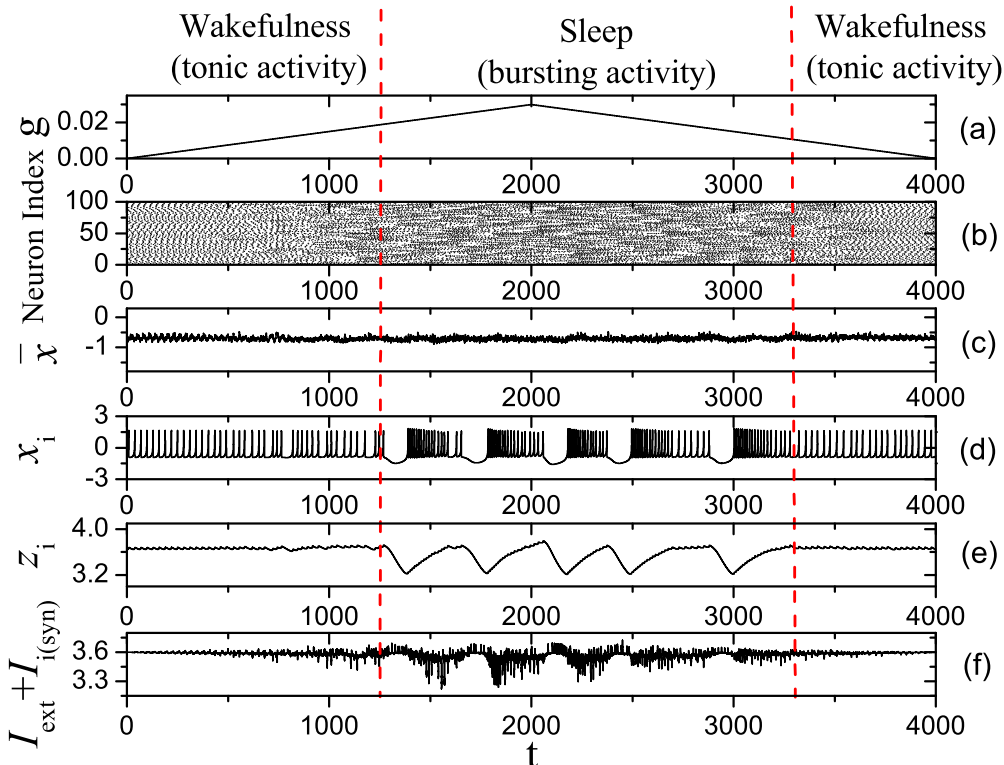


FIG. 9. The same as in Fig. 2, but for a chemically coupled network including both excitatory and inhibitory synapses at a ratio of 1:4.

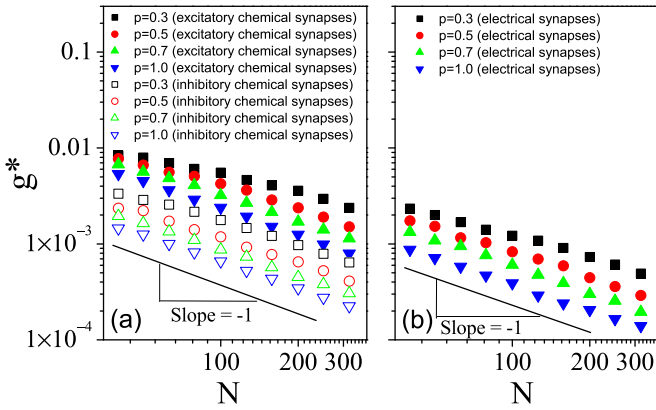


FIG. 10. The critical g^* as a function of N for different connection probabilities $p = 0.3, 0.5, 0.7, 1.0$ (i.e., globally coupled network) with chemical (a) or electrical (b) synapses. Data are averaged over ten realizations of the networks with random initial conditions. For comparison, the solid lines indicating the power-law property with an exponent of -1 are shown in (a) and (b).

larger than that in an electrically coupled network for the same \bar{k} .

In the following, we proceed to the theoretical analysis of the power-law relation (i.e., $g^* \sim \bar{k}^{-1}$) and explore the bursting response to the oscillatory input of a synaptic coupling current. In Eqs. (1) and (4), the synaptic coupling currents in the homogeneous ER networks, $I_{i(\text{syn})} = g \sum_{j=1, j \neq i}^N A_{ij}(V_s - x_j)G_j$ and $g \sum_{j=1, j \neq i}^N A_{ij}(x_j - x_i)$, are approximately proportional to the coupling strength g and the average number of signals that all the neurons receive (i.e., the network average degree \bar{k}). The synaptic current $I_{i(\text{syn})}$ for each neuron i can be regarded as an oscillating current with randomness [see Figs. 2(f), 4(f) and 6(f)]. In the homogeneous ER network with identical neurons, the $I_{i(\text{syn})}$ for each neuron i is approximately the same. As a result, each neuron can be approximately regarded as a single (or uncoupled) neuron characterized predominantly by the identical synaptic oscillating current I_{syn} , whose dynamics can approximately reflect the dynamics of some other neurons in the network. Thus, we focus on the dynamics of the single neuron dominant by the synaptic oscillating

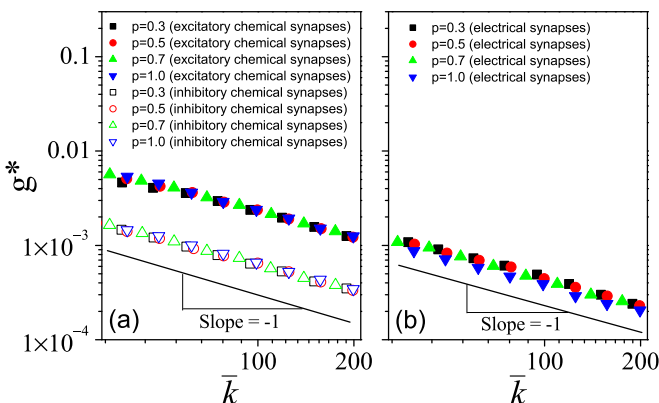


FIG. 11. The same as in Fig. 10, but as a function of the network average degree \bar{k} .

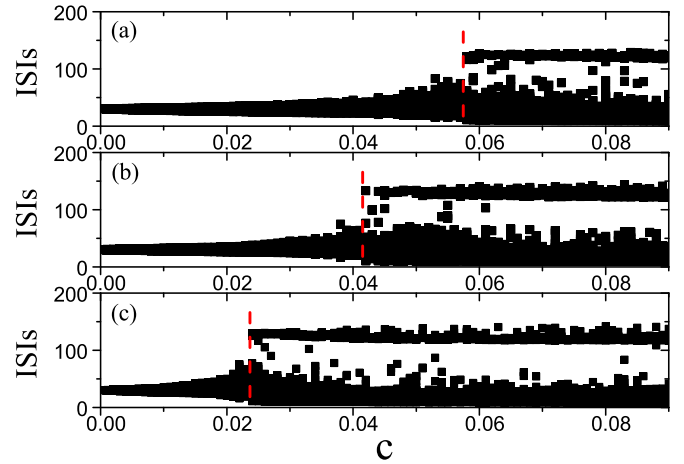


FIG. 12. The diagram of ISIs versus c at $\omega = 0.3$ for excitatory (a) or inhibitory (b) chemical synapses, and electrical synapses (c) in the presence of synaptic oscillating currents Eqs. (6)–(8), respectively. The vertical red dashed lines illustrate the critical c^* producing the transition between tonic and bursting activities.

lating current I_{syn} . We model the oscillating current as a simple type of fluctuation, consisting of a sinusoidal signal and a white noise. In a chemically coupled network with excitatory synapses, the synaptic oscillating current with positive value is given by

$$I_{\text{syn}} = g\bar{k}\{0.5[1 + \sin(\omega t)] + \xi\}. \quad (6)$$

For a chemically coupled network with inhibitory synapses, the synaptic oscillating current with negative value is as follows:

$$I_{\text{syn}} = -g\bar{k}\{0.5[1 + \sin(\omega t)] + \xi\}. \quad (7)$$

On the other hand, in an electrically coupled network, we adopt the synaptic oscillating current including the positive and negative values,

$$I_{\text{syn}} = g\bar{k}[\sin(\omega t) + \xi]. \quad (8)$$

In Eqs. (6) and (7), ξ is a white noise uniformly distributed between 0 and 1, and that between -1 and 1 in Eq. (8). The following results do not qualitatively depend on the value of ω and the distribution type of ξ . We adopt the parameter $c = g\bar{k}$, that reflects the oscillation amplitude of the synaptic current. In order to study the response of the neuron to the synaptic oscillatory input, a single neuron is hereby driven by such an oscillatory synaptic current I_{syn} . The dynamics of the single neuron can be described by the following equations:

$$\dot{x} = y - ax^3 + bx^2 - z + I_{\text{ext}} + I_{\text{syn}}, \quad (9)$$

$$\dot{y} = c - dx^2 - y, \quad (10)$$

$$\dot{z} = r[s(x - x_0) - z], \quad (11)$$

where the same parameters (including $I_{\text{ext}} = 3.6$) are adopted as in the above coupled networks [i.e., in Eqs. (1)–(4)]. By simulating the dynamics of the single neuron, we find that in Fig. 12, the transition from the tonic to the bursting activity can appear with the increasing of oscillation amplitude c , and

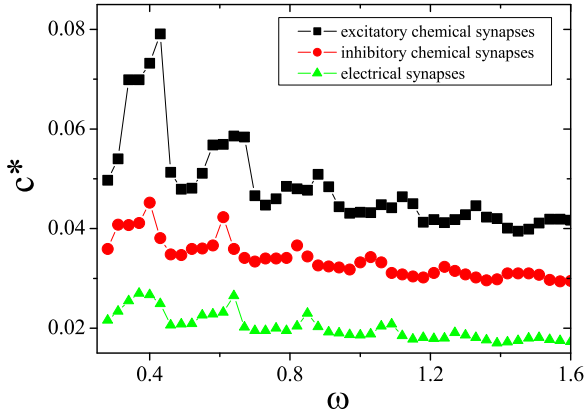


FIG. 13. The diagram of c^* versus ω for different synapses in the presence of corresponding synaptic oscillating currents. Data are averaged over ten realizations with random initial conditions.

that there is a critical constant c^* in the presence of the three types of synaptic oscillating currents, respectively. According to $c = g\bar{k}$, the dynamical transition can thus appear with the increasing of g , and there exists a critical g^* if the \bar{k} is fixed. Moreover, there is the relation $g^*\bar{k} = c^*$, being a constant for the different \bar{k} . Consequently, $g^* \sim \bar{k}^{-1}$ is obtained, and it verifies Eq. (5). Similarly, one can get the relation $g^* \sim \bar{k}^{-1}$ if the model of the synaptic oscillating current includes many sinusoidal signals with the different ω . Additionally, we show the critical constant c^* as a function of ω in Fig. 13. It is found that the c^* fluctuates as ω increases and that the amplitude of fluctuation decreases with the increasing of ω . As shown in Figs. 12 and 13, the critical constant c^* in the presence of excitatory chemical synapses is larger than that in the presence of inhibitory chemical synapses for the same ω . Moreover, the critical constant c^* in the presence of inhibitory chemical synapses is larger than that in the presence of electrical synapses for the same ω . According to $g^*\bar{k} = c^*$, the same relations of g^* apply with those of c^* for the different synapses, and thus, these can also be obtained for the fixed \bar{k} , consistently with the results of Fig. 11. As compared to the result of Fig. 1, one can see that the response of an HR neuron to the oscillatory input is very different to that to the static input. Indeed, the bursting activity in coupled networks results from the oscillation of the synaptic current.

IV. CONCLUSION AND DISCUSSION

To sum up, we investigated the neural activities and their transitions during the wakefulness-sleep cycle by using a simple model of coupled HR neurons in a homogeneous ER network. By tuning the synaptic strength, two spontaneous transitions between the tonic and the bursting neural activities are realized. The SWA resulting from the synchronized bursting activities during sleep can appear in the presence of excitatory chemical synapses (or electrical synapses). Meanwhile, the SWA cannot appear due to the emergence of desynchronized bursting activities when the inhibitory chemical synapses are dominant. In particular, the critical synaptic strength related to two transitions of the neural activities depends strongly on the network average degree. It was found

both numerically and analytically that they obey a power-law relation with an exponent of -1 .

Less is known about the mechanism underlying the slow (<1 Hz) oscillation that occurs during sleep in animals and humans [4,7]. So far, there have been many models of the thalamocortical slow-wave sleep oscillations [6,7], all of which reflect that the oscillations arise from an interaction between the cortical and the thalamic circuits. Based on the experimental association between the synaptic changes and the neural dynamical transitions throughout the wakefulness-sleep cycle, and by using our model of neural network, we found that, only the network coupling occurring under the changes of synaptic strength (that does not take into account the interaction between cortical and thalamic circuits) can contribute to the dynamical transitions at both the neuronal (tonic-burst) and the network (SWA) levels. Alternatively, our network model might provide a probable dynamical network mechanism for the SWA. By introducing the model of synaptic oscillating current, we found that the synchronized bursting activities and the resulting SWA are induced by synaptic oscillatory inputs in the presence of excitatory chemical synapses or electrical synapses. It is worth mentioning that the time unit of the model is a numerical simulation time unit (i.e., it has no explicit unit) according to the description in the original reference regarding the HR neuron [15]. The timescale is equivalent to millisecond. The SWA induced by the synchronized spike-burst activity in coupled HR neurons can describe the slow (<1 Hz) oscillations during sleep [18]. Additionally, the decaying time constants of the chemical synapses (with typical values for excitatory synapses being smaller than those for inhibitory ones) can impact the interburst intervals (results not shown), which have an impact on the onset and frequency of the collective oscillations, and might yield richer SWA. In the network, the oscillation of the synaptic coupling current results from the large synaptic strength g . In fact, the larger the g , the larger the amplitude of synaptic oscillating current, as shown in Figs. 2(f), 4(f), 6(f), 8(f), and 9(f). In this study, we focus on the analysis of $g^* \sim \bar{k}^{-1}$ by using the model of synaptic oscillating current with noise. The bursting activity induced by the synaptic oscillatory inputs might have been dependent on the amplitude and the frequency of the oscillation, as well as on the strength of the noise. The further dynamical analysis of the bursting activity induced by the synaptic oscillation remains an open and very interesting question.

It is noted that the transitions between the tonic and the bursting neural activities can also appear in the heterogeneous networks, such as in a scale-free network or a star network. However, the critical synaptic strength related to these transitions does not depend only on the network average degree, suggesting that some other network factors are more strongly influencing the transition in the heterogeneous network. In the future, we will investigate in detail the dependence of critical synaptic strength in these heterogeneous networks. Moreover, in order to focus on the role of synaptic strength in the production of two transitions between tonic and bursting neural activities, we herein considered identical neurons with the same synaptic strengths in the homogeneous ER network. In the future, when nonidentical neurons, different types of synapses (excitatory and inhibitory chemical, and electrical

synapses) and different synaptic strengths are collectively (or partially) considered in a heterogeneous (e.g., scale-free [23], modular [24], or hierarchical [24,25]) network for a more realistic neural systems' simulation, further investigations will be expected to produce the dynamic clusters of synchronized bursting activities with different interburst intervals, and thus could form richer SWAs similar to those found in experiments during sleep [26]. In the SWA up state, the synchronized spikes within the bursting activities might contribute to the sharp-wave ripples [27,28]. In particular, the different forms of synaptic plasticities [29,30] (e.g., short-term depression [31] and spike-timing-dependent plasticities [32–34]) characterized by the interplay between structure and dynamics, will

make the study of the transitions between the tonic and the bursting neural activities, and that of SWA, both interesting and challenging.

ACKNOWLEDGMENTS

This work was partially supported by National Natural Science Foundation of China under Grants No. 11875031 and No. 11975194; Scientific and Technological Activity Foundations for Preferred Overseas Chinese Scholar in Ministry of Human Resources and Social Security of China and in Department of Human Resources and Social Security of Anhui Province.

-
- [1] D. A. McCormick and H. R. Feeseer, *Neuroscience* **39**, 103 (1990).
 - [2] M. Steriade, A. Nuñez, and F. Amzica, *J. Neurosci.* **13**, 3252 (1993).
 - [3] S. Postnova, K. Voigt, and H. A. Braun, *J. Biol. Phys.* **33**, 129 (2007).
 - [4] M. Steriade, D. A. McCormick, and T. J. Sejnowski, *Science* **262**, 679 (1993).
 - [5] F. Amzica and M. Steriade, *Electroencephalogr. Clin. Neurophysiol.* **2**, 69 (1998).
 - [6] S. K. Esser, S. Hill, and G. Tononi, *J. Neurophysiol.* **102**, 2096 (2009).
 - [7] M. Bazhenov, I. Timofeev, M. Steriade, and T. J. Sejnowski, *J. Neurosci.* **22**, 8691 (2002).
 - [8] U. Olcese, S. K. Esser, and G. Tononi, *J. Neurophysiol.* **104**, 3476 (2010).
 - [9] G. F. Gilestro, G. Tononi, and C. Cirelli, *Science* **324**, 109 (2009).
 - [10] Z. Liu, U. Faraguna, C. Cirelli, G. Tononi, and X. Gao, *J. Neurosci.* **30**, 8671 (2010).
 - [11] G. Tononi and C. Cirelli, *Sleep Med. Rev.* **10**, 49 (2006).
 - [12] S. K. Esser, S. L. Hill, and G. Tononi, *Sleep* **30**, 1617 (2007).
 - [13] G. Tononi and C. Cirelli, *Brain Res. Bull.* **62**, 143 (2003).
 - [14] R. Huber, M. F. Ghilardi, M. Massimini, and G. Tononi, *Nature (London)* **430**, 78 (2004).
 - [15] J. L. Hindmarsh and R. M. Rose, *Proc. R. Soc. Lond. B* **221**, 87 (1984).
 - [16] C. Vreeswijk and H. Sompolinsky, *Science* **274**, 1724 (1996).
 - [17] T. P. Vogels and L. F. Abbott, *J. Neurosci.* **25**, 10786 (2005).
 - [18] M. Dhamala, V. K. Jirsa, and M. Ding, *Phys. Rev. Lett.* **92**, 028101 (2004).
 - [19] I. Belykh, E. de Lange, and M. Hasler, *Phys. Rev. Lett.* **94**, 188101 (2005).
 - [20] P. Erdős and A. Rényi, *Publ. Math. Inst. Hung. Acad. Sci.* **5**, 17 (1960).
 - [21] S. W. Ying, M. Futter, K. Rosenblum, M. J. Webber, S. P. Hunt, T. V. Bliss, and C. R. Bramham, *J. Neurosci.* **22**, 1532 (2003).
 - [22] V. V. Vyazovskiy, U. Olcese, E. C. Hanlon, Y. Nir, C. Cirelli, and G. Tononi, *Nature (London)* **472**, 443 (2011).
 - [23] A.-L. Barabási and R. Albert, *Science* **286**, 509 (1999).
 - [24] D. Meunier, R. Lambiotte, and E. T. Bullmore, *Front. Neurosci.* **4**, 200 (2010).
 - [25] C. Zhou, L. Zemanová, G. Zamora, C. C. Hilgetag, and J. Kurths, *Phys. Rev. Lett.* **97**, 238103 (2006).
 - [26] S. Diekelmann and J. Born, *Nat. Rev. Neurosci.* **11**, 114 (2010).
 - [27] G. Buzsáki, *Hippocampus* **25**, 1073 (2015).
 - [28] Y. Norman, E. M. Yeagle, S. Khuvis, M. Harel, A. D. Mehta, and R. Malach, *Science* **365**, eaax1030 (2019).
 - [29] L. Abbott and W. Regehr, *Nature (London)* **431**, 796 (2004).
 - [30] S. J. Martin, P. D. Grimwood, and R. G. M. Morris, *Annu. Rev. Neurosci.* **23**, 649 (2000).
 - [31] L. F. Abbott, J. A. Varela, K. Sen, and S. B. Nelson, *Science* **275**, 221 (1997).
 - [32] J.-F. Zhou, W.-J. Yuan, D. Chen, B.-H. Wang, Z. Zhou, S. Boccaletti, and Z. Wang, *Phys. Rev. E* **99**, 032419 (2019).
 - [33] S. Song, K. D. Miller, and L. F. Abbott, *Nat. Neurosci.* **3**, 919 (2000).
 - [34] K. T. Li, J. Liang, and C. Zhou, *Neural Plast.* **2021**, 6668175 (2021).